CCIT Report #413 January 2003

Lateral and Longitudinal Coupled Waveguides in Semiconductor Lasers

O. Skorka and J. Salzman

O. Skorka and J. Salzman (*Department of Electrical Engineering, Microelectronics center and Solid State Institute, Technion, 32000, Haifa, Israel*)

E-mail: orsk@tx.technion.ac.il

Abstract: A semiconductor laser including two laterally coupled waveguides and a partially reflecting surface in one of the waveguides (an internal mirror) is analyzed. The spectrum of Fabry Perot modes at lasing threshold is drastically affected by the combined coupled-cavity effect.

Introduction: Semiconductor laser cavities formed by two parallel coupled waveguides have been studied [1-2]. The problem of two longitudinally coupled cavity lasers has also been investigated [3-5]. However, the case of a laser system, which exhibits both longitudinal and lateral coupling, has never been discussed. This problem has a significant experimental value in *GaN*-based lasers. The basic structure of *GaN*-based lasers includes a thick *GaN* layer grown on a substrate (sapphire or *SiC*) and a waveguide formed by *AlGaN* claddings, a *GaN* core and an *InGaN*-*GaN* multi-quantum-well (*MQW*) and high refractive index multi-layer [6]. The *AlGaN* refractive index is lower than the refractive index of its surrounding layers,thus, a parasitic *GaN* waveguide, parallel to the active waveguide is formed underneath the GaN laser. In addition to that, typical *GaN* layers exhibit threading dislocations with highest density near the film-substrate interface decreasing to 10^8-10^9cm^{-2} near the film surface. These extended defects merge into hexagonal hillocks [6]. The boundaries of those hexagons may present a slight reflectance; therefore, they can be regarded as internal mirrors. The analysis presented here has, however, a general applicability.

Device Analysis: The laser device under consideration is illustrated in Fig. 1. It consists of two parallel waveguides with a total length of $L_{tot} = L_1+L_2$. The lower waveguide, *WG-II*, includes an internal mirror, located at distance L_1 from $z=0$. There is no internal mirror in the upper waveguide, *WG-I*. The reflectance of each one of the mirrors is marked as $r_i(z)$, where i represents the waveguide index (i = I or II). The internal transmittance is $t_i(z)$. Neglecting the scattering losses at the mirrors, we take $t_i(\mathrm{z}) = \sqrt{1-r_i^2(\mathrm{z})}$.

At any fixed point of the cavity, the guided field of the coupled waveguides can be regarded either as a superposition of two individual channel modes (CM) or as composed of two system supermodes (SM). We use here the CM representation. The CM and the SM representations are interchangeable; the transformation between them can be performed by a matrix formalism presented in [1].

We define $a^f{}_i(z)$ and $a^b{}_i(z)$ as the amplitudes of the CM modes traveling in the $+z$ and $-z$ direction, with propagation coefficients β_I and β_{II}, respectively (defining $\beta_{av} \equiv (\beta_I + \beta_{II})/2$, $\Delta\beta \equiv (\beta_I - \beta_{II})/2$ and $\kappa^2 = \kappa_{I,II} \cdot \kappa_{II,I}$, $\kappa_{i,j}$ being the coupling coefficients between waveguide i and j). In the following, we use 2D vectors, $\underline{\boldsymbol{a}}^f(\mathrm{z}) = \begin{pmatrix} a_I^f(\mathrm{z}) \\ a_{II}^f(\mathrm{z}) \end{pmatrix}$, and $\underline{\boldsymbol{a}}^b(\mathrm{z}) = \begin{pmatrix} a_I^b(\mathrm{z}) \\ a_{II}^b(\mathrm{z}) \end{pmatrix}$.

The reflectance and transmittance operators at any discontinuity are given by:

1. $$\underline{\underline{\boldsymbol{R}}}(z) = \begin{pmatrix} r_I(z) & 0 \\ 0 & r_{II}(z) \end{pmatrix}, \quad \underline{\underline{\boldsymbol{T}}}(z) = \begin{pmatrix} t_I(z) & 0 \\ 0 & t_{II}(z) \end{pmatrix}$$

The propagation constants in SM are $\sigma_{1,2} = \beta_{av} \pm S$, where $S \equiv \sqrt{\kappa^2 + \Delta\beta^2}$. The propagation matrix over a section, Δz, is given by [1]:

2. $$\underline{\underline{\boldsymbol{P}}}(\Delta z) = \begin{pmatrix} p_1^2 e^{-i\sigma_1 \Delta z} + p_2^2 e^{-i\sigma_2 \Delta z} & p_1 p_2 (e^{-i\sigma_2 \Delta z} - e^{-i\sigma_1 \Delta z}) \\ p_1 p_2 (e^{-i\sigma_2 \Delta z} + e^{-i\sigma_1 \Delta z}) & p_1^2 e^{-i\sigma_2 \Delta z} - p_2^2 e^{-i\sigma_1 \Delta z} \end{pmatrix}$$

where $p_{1,2}^2 = (1 \pm \Delta\beta \ / S)/2$.

We look at two round trip loops in our structure: the first loop is taken from $z=L_1^-$ to $z=0$ and back and the second is taken from $z= L_1^+$ to $z= L_{tot}^-$ and back. Boundary conditions must be fulfilled in the transition between $z= L_1^+$ and $z= L_1^-$. From the first loop we get the following relation:

3. $$\underline{\boldsymbol{a}}^b(L_1^+) = \underline{\underline{\boldsymbol{S}}}\,\underline{\boldsymbol{a}}^f(0^+)$$

where $\underline{\underline{\boldsymbol{S}}} = \underline{\underline{\boldsymbol{S}}}_1^{-1}\underline{\underline{\boldsymbol{S}}}_2$, $\underline{\underline{\boldsymbol{S}}}_1 = \underline{\underline{\boldsymbol{R}}}(0^+)\underline{\underline{\boldsymbol{P}}}(L_1)\underline{\underline{\boldsymbol{T}}}(L_1^+)$, $\underline{\underline{\boldsymbol{S}}}_2 = \underline{\underline{\boldsymbol{I}}} - \underline{\underline{\boldsymbol{R}}}(0^+)\underline{\underline{\boldsymbol{P}}}(L_1)\underline{\underline{\boldsymbol{R}}}(L_1^-)\underline{\underline{\boldsymbol{P}}}(L_1)$ and $\underline{\underline{\boldsymbol{I}}}$ is the 2×2 identity matrix. From the second loop we obtain:

4. $$\underline{\boldsymbol{a}}^b(L_1^+) = \underline{\underline{\boldsymbol{M}}}\,\underline{\boldsymbol{a}}^f(0^+)$$

where $\underline{\underline{\boldsymbol{M}}} = \underline{\underline{\boldsymbol{M}}}_1^{-1}\underline{\underline{\boldsymbol{M}}}_2$, $\underline{\underline{\boldsymbol{M}}}_1 = \underline{\underline{\boldsymbol{I}}} - \underline{\underline{\boldsymbol{P}}}(L_2)\underline{\underline{\boldsymbol{R}}}(L_{tot}^-)\underline{\underline{\boldsymbol{P}}}(L_2)\underline{\underline{\boldsymbol{R}}}(L_1^+)$ and

$\underline{\underline{\boldsymbol{M}}}_2 = \underline{\underline{\boldsymbol{P}}}(L_2)\underline{\underline{\boldsymbol{R}}}(L_{tot}^-)\underline{\underline{\boldsymbol{P}}}(L_2)\underline{\underline{\boldsymbol{T}}}(L_1^-)\underline{\underline{\boldsymbol{P}}}(L_1)$.

From Eq. 3 and Eq. 4 we conclude that $\underline{\boldsymbol{a}}^f(0^+) = \underline{\underline{\boldsymbol{S}}}^{-1}\underline{\underline{\boldsymbol{M}}}\,\underline{\boldsymbol{a}}^f(0^+)$, therefore, for the existence of a non-trivial solution for $\underline{\boldsymbol{a}}^f(0^+)$, we require:

5. $$\left|\underline{\underline{\boldsymbol{S}}}^{-1}\underline{\underline{\boldsymbol{M}}} - \underline{\underline{\boldsymbol{I}}}\right| = 0$$

The roots to Eq. 5 determine the lasing wavelengths, λ_{FP}, and the threshold gain $g_i(\lambda_{FP})$ of the longitudinal Fabry-Perot (FP) modes, respectively. Within this simplified model, the gain provided by the MQW is introduced as an imaginary part of σ_s $(s=1,2)$:

6. $$\tilde{\sigma}_s = \sigma_{s,\mathrm{Re}} + j\sigma_{s,\mathrm{Im}}$$

Where $\sigma_{s,Re}$ is the σ_s value of the passive waveguides and

7. $$\sigma_{s,\mathrm{Im}} = \frac{1}{2}\left[\Gamma_s(\lambda_{FP})\cdot g_m(\lambda_{FP}) + (1-\Gamma_s(\lambda_{FP}))\alpha_m\right]$$

$\Gamma_s(\lambda_{FP})$ is the confinement factor of the *s* supermode into the MQW region at λ_{FP} and α_m represents the material losses (assuming the losses are not wavelength or location dependent).

Numerical Modeling: In this section we refer to a typical *GaN* laser structure [6]. The whole structure is described at Table 1. The substrate layer is sapphire, the coupling layer is $Al_{0.07}Ga_{0.93}N$ (layer 3 in table 1) and the upper cladding layer is air. We regard the structure formed by the substrate and by layers *1, 2 and 3* as *WG-II* and the structure of layers *4-9* as *WG-I*. The refractive indices of layers *1-9* were taken in accordance to [7], the temperature was assumed to be *350K*. The parameters used in our calculations are presented in Table 2. The refractive indices of the substrate and the upper cladding layer were taken constant as *1.68* and *1*, respectively.

In the model, the "laser active" waveguide, *WG-I*, is a single mode waveguide and its mode couples to the third mode of *WG-II*, the *GaN* waveguide. We consider here the particular case in which there is no internal mirror in *WG-I*: $r_I(L_I)=0$ and $t_I(L_I)=1$. Using our analysis along with the mentioned system parameters, we found the wavelengths, λ_{FP}, for which the condition defined by Eq. 5 takes place for a certain material gain. The material gain values at each one of those wavelengths are presented on Fig. 2. Those values exhibit a sinusoidal envelope, which may explain the spectrum often observed in this type of lasers [6].

In order to learn more about the effects of the internal mirror we changed the reflectivity of this mirror and its location. Changing the reflectivity affected only the modulation amplitude of the material gain required for lasing, Δg_m, the modulation depth increases with the reflectivity. For reflectivity changes in the range of *0.5-25%* we obtained a nearby constant product $\Delta g_m / r_{II}(L_1^-) \approx 1450cm^{-1}$. Changing the location of the mirror at *WG-II* affected the periodicity of the modulated gain spectrum, $\Delta\lambda$, the periodicity becomes shorter when the minimal distance between the internal mirror and its proximal facet increases. For L_2 changes in the range of $10\text{-}150\mu m$ a $\Delta\lambda$ times L_2 product, $\Delta\lambda \cdot L_2 \approx 24.1 nm\mu m$, was obtained.

Conclusions: In this work, a model for a longitudinal and lateral coupled cavity laser was presented. This model provides a tool to determine the lasing wavelengths and the material gain required at each Fabry-Perot mode. The output results of a simulation, which used *GaN*-based lasers parameters, may be used to understand experimental results and to draw conclusions about non-ideal factors influencing *GaN*-based lasers.

Acknowledgment: This work was supported by the Israel Academy of Science and by the Fund for Promotion of Research at the Technion.

References

1. R. Lang, A. Yariv and J. Salzman, "Laterally Coupled Cavity Semiconductor Lasers," IEEE Journal of Quantum Electronics, Vol. QE-**23**, No. 4, 395-400 (1987).
2. I. A. Avrutsky, R. Gordon, R. Clayton, and J. M. Xu "Investigation of the spectral characteristics of 980-nm InGaAs-GaAs-AlGaAs Lasers" IEEE J. Quantum Electron. **33,** 1801 (1997).
3. C. H. Henry and R.F. Kazarinov, "Stabilization of Single Frequency Operation of Coupled-Cavity Lasers", IEEE Journal of Quantum Electronics, Vol. QE-**20**, No. 7, 733-744 (1984).
4. K. J. Ebeling and L.A. Coldren "Analysis of Multielement Semiconductor Lasers" J. Appl. Phys. Vol. **54**, No. 6, 2962-2969 (1983).
5. L. A. Coldren and T. L. Koch "Analysis and Design of Coupled-Cavity Lasers" (two parts) IEEE J. of Quantum Electronics, Vol. QE-**20**, No. 6, 659-682 (1984).
6. S. Nakamura and G. Fasol, *The Blue Laser Diode* (Springer, Berlin, 1997).
7. U. Tisch, B. Meyler, O. Katz, E Finkman and J. Salzman, "The Depence of the Refractive Index of $al_xGa_{1-x}N$ on Temperature and Composition at Elevated Temperatures" J. Appl. Phys.**89**, 2676 (2001).

Figure Captions

Fig. 1 Schematic drawing of the coupled-cavity laser formed by the two parallel waveguides, *WG-I* and *WG-II,* with an internal mirror in *WG-II*.

Fig. 2 Material gain vs. wavelength at wavelengths for which the eigenvalue condition, Eq. 5, is fulfilled. The calculation parameters appear in Table 2.

Table Captions

Table 1 The layers of the laser used for the calculations.

Table 2 The simulation parameters.

Table 1

Layer No.	*Layer*	*Layer thickness*
Substrate	*Sapphire*	
1	GaN	3μm
2	$In_{0.05}Ga_{0.95}N$	0.1μm
3	$Al_{0.07}Ga_{0.93}N$	0.5μm
4	GaN	0.1μm
5	MQW=4×($In_{0.15}Ga_{0.85}N(d_h)+In_{0.02}Ga_{0.98}N(d_l)$)	d_h = 35Å, d_l = 70Å
6	$Al_{0.2}Ga_{0.8}N$	200Å
7	GaN	0.1μm
8	$Al_{0.07}Ga_{0.93}N$	0.5μm
9	GaN	0.2μm

Table 2

$r_I(0^+)$	$r_{II}(0^+)$	$r_I\ (L_1^-)$	$r_{II}(L_1^-)$	$r_I(L_{tot}^-)$	$r_{II}(L_{tot}^-)$	L_2	L_{tot}	$\kappa \equiv \sqrt{\kappa_{I,IIj}\kappa_{II,Ij}}$	α_m
1	1	0	0.02	0.467	0.444	80μm	500μm	100cm^{-1}	10cm^{-1}

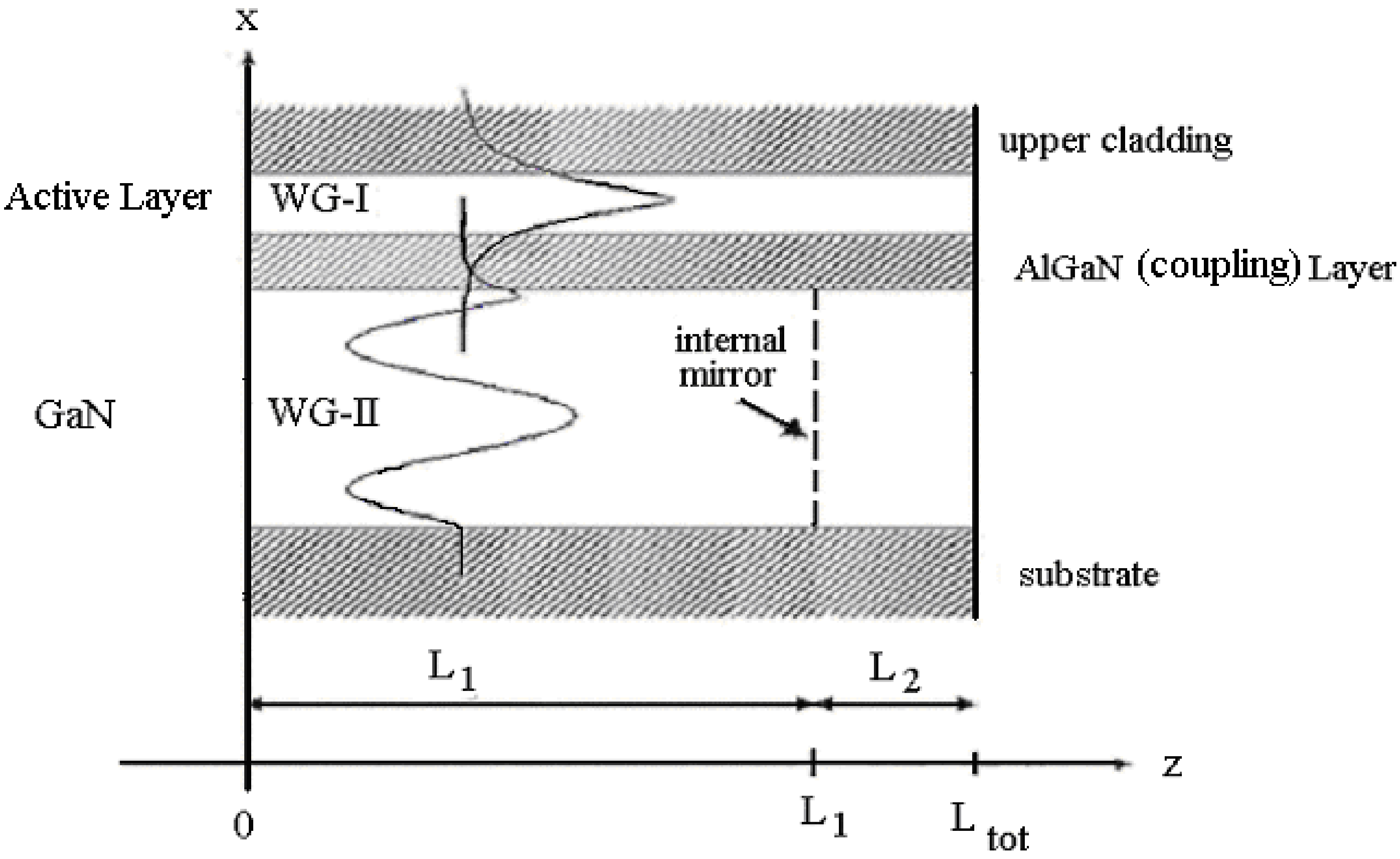
x
upper cladding
Active Layer
WG-I
AlGaN (coupling) Layer
internal
mirror
GaN
WG-II
substrate
L1
L2
z
0
L1
L tot

Figure.1

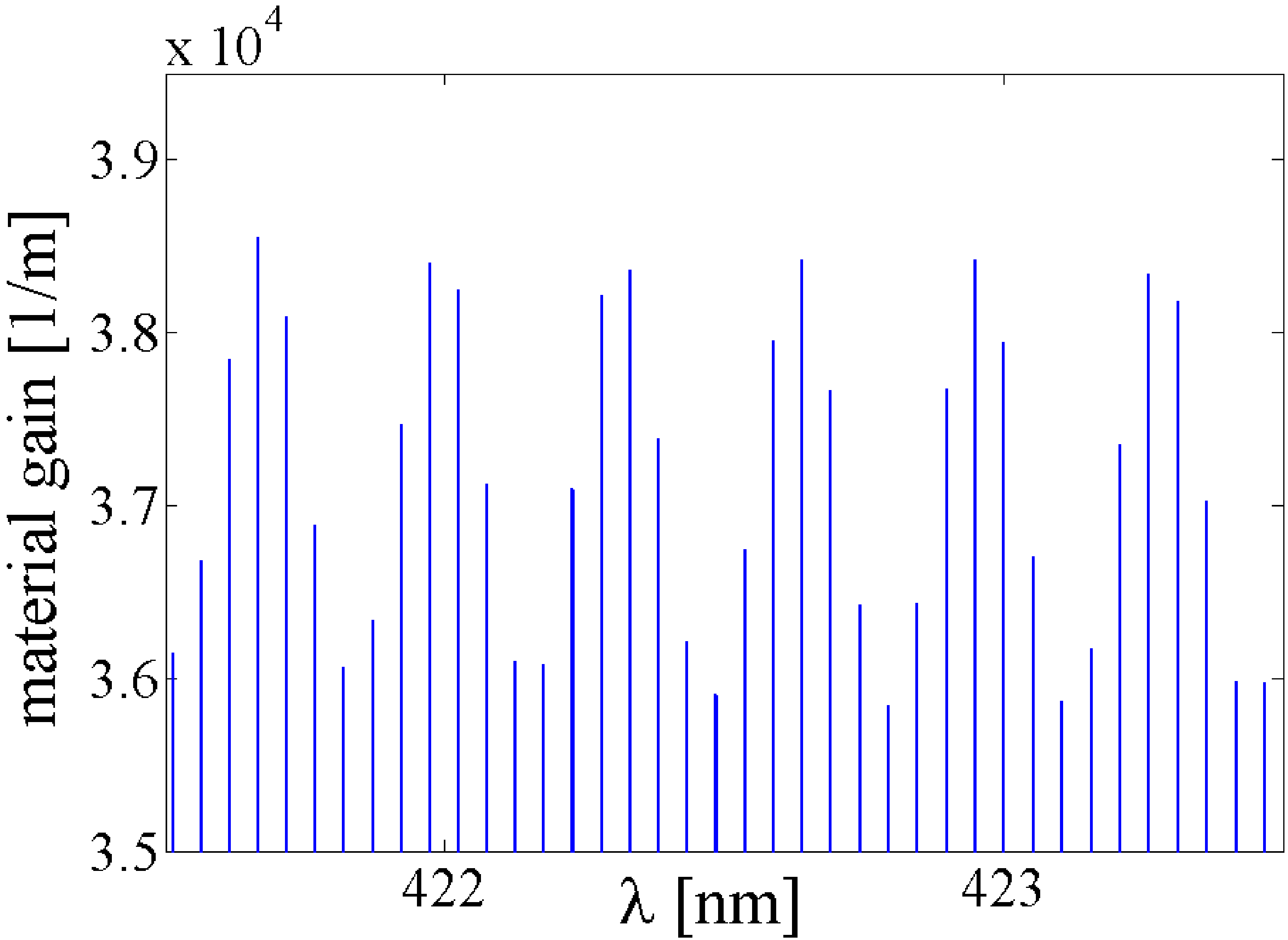

Figure.2